Stability of Proteins Encapsulated in Michael-Type Addition Polyethylene Glycol Hydrogels

Zahra Ghassemi[1,#], Sam Ruesing[2,#], Jennie B Leach[1,*], Silviya P Zustiak[2,*]

[1]Chemical, Biochemical, and Environmental Engineering, University of Maryland, Baltimore County, 1000 Hilltop Circle, Engineering 314, Baltimore, MD 21250, USA.

[2]Biomedical Engineering, Saint Louis University, 3507 Lindell Blvd, St. Louis, MO 63103, USA.

[#]Indicates equal contribution

*To whom correspondence should be addressed:

Silviya P Zustiak

Biomedical Engineering Program

Saint Louis University

St. Louis, MO 63103-2010

Phone: 314-977-8331

Email: silviya.zustiak@slu.edu

Jennie B Leach

Chemical, Biochemical, and Environmental Engineering Department

University of Maryland, Baltimore County,

Baltimore, MD 21250

Phone: 410-455-8152

Email: jleach@umbc.edu

Abstract

Degradable polyethylene glycol (PEG) hydrogels are excellent vehicles for sustained drug release due to their biocompatibility, tunable physical properties, and customizable degradation. However, protein therapeutics are unstable under physiological conditions and releasing degraded or inactive therapeutics can induce immunogenic effects. While controlling protein release from PEG hydrogels has been extensively investigated, few studies have detailed protein stability long-term or under stress conditions. Here, lysozyme and alcohol dehydrogenase (ADH) stability were explored upon encapsulation in PEG hydrogels formed through Michael-Type addition. The stability and structure of the two model proteins were monitored by measuring free energy of unfolding and fluoresce quenching when confined in a hydrogel and compared to PEG solution and buffer. Hydrogels destabilized lysozyme structure at low denaturant concentrations but prevented complete unfolding at high concentrations. ADH was stabilized as the confining mesh size approached the protein radius of gyration. Both proteins retained enzymatic activity within the hydrogels under stress conditions, including denaturant, high temperature, and agitation. Conjugation between lysozyme and PEG-acrylate was identified at long reaction times but no conjugation was observed in the time required for complete gelation. Studies of protein stability in PEG hydrogels, as the one detailed here, can lead to designer technologies for improved formulation, storage, and delivery of protein therapeutics.

Key words: poly(ethylene) glycol, hydrogels, drug delivery, protein stability, confinement

1. Introduction

Polyethylene glycol (PEG) hydrogels have shown promise as a biomaterial for biotherapeutic delivery (Li & Mooney, 2016). They are appealing due to their physical similarities to native tissue as well as their biocompatibility, modulus, versatility and high water content (typically 70-90%) (Bryant, Bender, Durand, & Anseth, 2004). PEG hydrogels can be made degradable via the incorporation of hydrolytically-degradable synthetic crosslinkers (Silviya P. Zustiak & Leach, 2010) or enzymatically-degradable peptide crosslinkers (Lutolf et al., 2003), which negates the need for device removal. When used as biotherapeutic delivery devices, proteins are typically encapsulated within the hydrogel through entrapment or chemical conjugation (Jain, Sheth, Dunn, Zustiak, & Sell, 2017). As biotherapeutics proteins are susceptible to physical and chemical damage *in vivo*, reducing their effectiveness and triggering a heightened immune response via protein aggregates (Rosenberg, 2006). However, confinement within a hydrogel is predicted to have stabilizing effects. For example, several globular proteins, including lysozyme, myoglobin, bovine serum albumin, alpha-lactalbumin, apomyoglobin and faxitin, have been shown to be stabilized in confinement in gels and sol-gels *in vitro* (Bolis, Politou, Kelly, Pastore, & Temussi, 2004; Eggers & Valentine, 2001; Nakano, Yamaguchi, & Sugimoto, 2018).

The effects of confinement on protein folding have been investigated by theoretical (Minton, 1992, 2006; Zhou, Rivas, & Minton, 2008), computational studies (Cheng et al., 2018; Chu, Suo, & Wang, 2020; Xu, Cheng, Wu, Liu, & Li, 2017), and experimental studies (Asuri & Kunkel, 2014; Simpson, Szeto, Boukari, Good, & Leach, 2020; Wang & Akcora, 2017), but significant disagreement exists between the results of these studies. For PEG hydrogels in particular, much research has been focused on controlling protein release (Bhattarai, Ramay, Gunn, Matsen, & Zhang, 2005; Kharkar, Kloxin, & Kiick, 2014; Lin & Anseth, 2009; Van de Wetering, Metters, Schoenmakers, & Hubbell, 2005), but few have focused on protein stability and structure long-

term or under stress conditions (Simpson et al., 2020). Such detailed investigations will enable the translation of PEG hydrogels as biotherapeutic delivery devices.

Here, PEG hydrogels were fabricated via a step-growth Michael-type addition between acrylate and thiols, generating a relatively homogeneous network. This particular PEG hydrogel chemistry is a promising candidate for embedding protein therapeutics because: (i) drug release can be sustained and controlled by PEG degradation and swelling rates; (ii) the mesh size of a PEG hydrogel (~10-20 nm) and can be tuned by changing the concentration, molecular weight, and the number of arms on PEG derivatives (Silviya P. Zustiak & Leach, 2010); and (iii) the formulation is injectable and protein can be encapsulated prior to gelation ensuring high loading and homogeneous distribution (Jain et al., 2020). In contrast to other crosslinking chemistries (i.e., photoinitiated chain-growth polymerizations), Michael-type addition reactions do not form free radicals that may lead to protein denaturation. Nevertheless, the presence of acrylate and thiol groups may disrupt the native structure, specifically disulfide bonds of encapsulated proteins, and induce protein denaturation (Lin & Anseth, 2009; Nair et al., 2014).

As a step towards optimizing the effectiveness of hydrogels as protein delivery devices and tissue engineering scaffolds, the goal of this study was to evaluate the molecular-level effects on protein structure and function upon encapsulation in a PEG hydrogel. Specifically, we focused on the model proteins lysozyme and alcohol dehydrogenase, to investigate the effect of hydrogel crosslinking and confinement on protein bioactivity and thermodynamic stability at mild stress conditions as measured by free energy of unfolding and fluorescence quenching. We report that lysozyme and alcohol dehydrogenase structure and activity were affected neutrally or beneficially upon encapsulation and confinement in PEG hydrogels versus solution in most conditions, except for higher PEG gel concentrations where the gel mesh size approached the protein size to provide a high confinement environment.

2. Materials and Methods

2.1. Materials

Polyethylene glycol (PEG-OH; 6 kDa) was obtained from Alfa Aesar (Haverhill, MA). PEG-diacrylate (PEG-DA; 5 kDa), 4-arm PEG-acrylate (4-arm PEG-Ac; 10 and 20 kDa), PEG-dimethacrylate (PEG-DM; 1 kDa), and PEG-dithiol (PEG-diSH; 3.4 and 10 kDa) were from Laysan Bio Inc. (Arab, Al). Hen egg-white lysozyme (Lys), alcohol dehydrogenase from *Saccharomyces cerevisiae* (ADH), phosphate buffered saline (PBS), dithiothreitol (DTT) and triethanolamine (TEA) were from Millipore Sigma (Burlington, MA). Silicone isolator sheets (0.5 mm thick), from Grace Bio Labs (Bend, OR), were used as spacers. Guanidinium hydrochloride (GuHCl), ethanol, tris hydrochloride, NuPAGE, Novex, and SimplyBlue Safestain, and Pierce In-Solution Tryptic Digestion and Guanidination were from Thermo Fisher Scientific (Waltham, MA). Barium chloride, iodine, and perchloric acid were from Fisher Chemicals (Hampton, NH). TopSeal-A PLUS was from (PerkinElmer, Waltham, MA). Guanidine thiocyanate (GuSCN) was from Promega (Madison, WI). β-Nicotinamide-adenine dinucleotide (NAD^+) was from Calbiochem (San Diego, Ca). A kit from Biovision (Milpitas, CA) was used to measure lysozyme activity.

2.2. Hydrogel Fabrication

Stock solutions of ADH and Lys (5 mg/mL), 4-arm PEG-Ac (20% w/v), and PEG-diSH (20% w/v) were prepared in 0.3 M TEA in PBS, pH 7.4 (TEA buffer). The stock solutions were then used to prepare a hydrogel precursor solution of 0.5 mg/mL Lys and 10% w/v PEG or 0.5 mg/mL ADH and 5, 7.5, 10, 12.5, or 15% w/v PEG with stoichiometrically equal acrylate and thiol groups. The precursor solution was mixed by gentle pipetting and incubated at room temperature for 45 min (Lys) - 120 min (ADH) to allow gelation.

2.3. Mesh Size

The mesh size (ξ) of hydrogels was determined according to the Flory-Rehner theory as described by us previously (Silviya P. Zustiak & Leach, 2010). Hydrogel mass was measured immediately following fabrication to obtain the relaxed mass (M_R). The gels were then placed in PBS for 1 hr before reweighing to determine the swollen mass (M_S). The gels were then dried overnight in a 60 °C oven and reweighed to determine the dry mass (M_D). ξ was then calculated as [27]:

$$\xi = (\upsilon_{2,s})^{-\frac{1}{3}} \left(\frac{2C_n\overline{M_c}}{M_r}\right)^{\frac{1}{2}} l \quad (1)$$

where $v_{2,s}$ is the polymer volume fraction in the swollen state, C_n is the characteristic ratio for PEG, M_C is the average molecular weight between two crosslinks, M_r is the molecular weight of a PEG repeat unit, and l is the bond length between the C-C and C-O in a PEG repeat unit.

2.4. Non-Reduced SDS PAGE and Native PAGE

Lys and AHD at 0.5 mg/mL were incubated in TEA buffer (control) and 10% w/v PEG solutions: 4-arm PEG-Ac, PEG-diSH, PEGDA, PEG-MAL, and PEG-OH, for up to 24 hrs at room temperature. After incubation, samples were prepared according to the manufacturer's protocols for non-reduced SDS PAGE and native PAGE. SDS PAGE was performed at constant 200 V for 40 min on a Bis-Tris 4-12% gradient gel. Native PAGE was performed at constant 225 V for 90 min on a Tris-Glycine 4-20% gradient gel. PAGE gels were run in an XCell SureLock cell (Thermo Fisher, Waltham, MA) powered by a PowerPac Basic power supply (Bio-Rad, Hercules, CA). For Lys, due to the lysozyme's positive charge at the Bis-Tris running buffer pH, Native PAGE was run with reversed electrode polarity. Lanes were loaded with sample volume corresponding to 5 and 2.5 µg of protein for SDS and Native PAGE, respectively. Gels were stained with SimplyBlue

Safestain for protein and Barium Iodine for PEG (Natarajan, Xiong, Albrecht, DeNardo, & DeNardo, 2005).

2.5. Rheology

Gel precursor solution was prepared as described previously and pipetted onto a rheometer stage (AR 2000ex rheometer, TA Instruments, New Castle, DE). The storage modulus (*G'*) was monitored using parallel-plate geometry with oscillation frequency of 1 Hz, strain of 2%, and gap height of 400 μm. Each gel solution (130 μL) was monitored for 3000 sec at room temperature. The evolution in *G'* was fit to the Hill equation to give effective gelation time (Calvet, Wong, & Giasson, 2004):

$$G'(t) = G'_{\infty}\left(\frac{1}{1+\left(\frac{t_{gelation}}{t}\right)^{m}}\right) \quad (2)$$

where $t_{gelation}$ is the time required to achieve half of the steady-state storage modulus (G'_{∞}) and *m* is the Hill coefficient related to the slope of the gelation curve.

2.6. High Resolution Mass Spectrometry

Stock solutions were prepared by dissolving lysozyme and 4-arm PEG-Ac in LC/MS grade water at 1:1 (0.5 mg/mL lysozyme and 0.5 mg/mL 4-arm PEG-Ac) and 1:20 (2 mg/mL lysozyme and 40 mg/mL 4-arm PEG-Ac) mass ratio and incubated for 1 and 44 hrs prior to analysis. High resolution mass spectrometry was performed on a Bruker Daltonics SolariX Fourier transform ion cyclotron resonance mass spectrometer equipped with a 12 Tesla actively shielded superconducting magnet and electrospray Ionization (ESI) source. Working solutions were prepared by diluting stock solutions in LC/MS grade water to a concentration of 0.01 mg/mL lysozyme alone or in 0.01 or 0.20 mg/mL 4-arm PEG-Ac, then introduced to the ESI source at 10 μL/min via a syringe pump.

ESI source conditions for the capillary and end plate offset were 4500 V and -500 V, respectively. Source gas (N_2) conditions were 3.5 bar nebulizer, 4.0 L/min dry gas, and 200°C dry temperature.

To determine the lysozyme fragments that react with PEG, a stock solution was prepared by dissolving lysozyme (2 mg/mL) and 4-arm PEG-Ac (40 mg/mL) in LC/MS grade water and allowed to react at 25°C for 1 hr. Lysozyme (2 mg/mL) in LC/MS grade water was used as control. The Pierce In-Solution Tryptic Digestion and Guanidination Kit was utilized to alkylate and digest lysozyme and then guanidinate the peptide fragments. Digested samples were diluted 1:400 into LC/MS grade water, 2% acetonitrile and 0.1% formic acid and placed into Microsolv 9512S-3CP-RS RSA 1.8 ml vials and loaded into the Bruker NanoElute HPLC having a Bruker FIFTEEN ReproSil C18 # 1842621 column for separation and infused with a flow rate of 500 nL/min directly into the Bruker timsTOF pro Mass Spectrometer (Billerica, MA) for mass spec analysis. The mass spectrometer was equipped with a Captive Spray Ionization (CSI) source used in positive mode, mass range from 100-1700 m/z, capillary set to 1700 volts, drying gas 3.0 L/min, 180°C dry temperature, PASEF Fragmentation mode, and time setting on 0.85-1.0 V-S/cm^2. Thermo Fisher Scientific Sequencing Analysis Software v5.3 and BioInformatics Solutions (Waterloo, Ontario, Canada) PEAK studio 10.5 were used for data analysis.

2.7. Free Energy of Unfolding

A hydrogel precursor solution with 0.5 mg/mL Lys was pipetted into UV-star clear bottom 96-well plates at 70 µL per well. After 45 mins of gelation, 70 µL of denaturant (GuSCN, 0–3 M) was added to each well. For ADH, a hydrogel precursor solution with 0.5 mg/mL ADH was pipetted into UV-star clear bottom 96-well plates at 70 µL per well. After 120 min of gelation, 45, 55, 70, 95, 115 µL of denaturant (GuHCl, 0–4 M) was added to each well of 5, 7.5, 10, 12.5, and 15% w/v PEG, respectively. Plates were covered with TopSeal-A PLUS and mixed on a Sartorius CERTOMAT BS-1 orbital shaking incubator (Göttingen, Germany) at 23 °C and 150 RPM for 2

hrs for Lys and 100 RPM for 4 hrs for ADH. Then, the intrinsic fluorescence intensity (Ex. 295 nm, Em. 300–400 nm, 2 nm steps) of lysozyme in the presence of denaturant was measured on a Spectra Max M5 with SoftMax Pro Software (Molecular Devices, San Jose, CA) at 23 °C. Energy of unfolding was calculated from solvent denaturation curves using the linear extrapolation method (Pace & Shaw, 2000). Briefly, the equilibrium constant (*K*) was calculated from the solvent denaturation curve data using $\boldsymbol{K = [(Y)_N - (Y)]/[(Y) - (Y)_D]}$, where $\boldsymbol{(Y)}$ is the wavelength of the maximum emission intensity, and $\boldsymbol{(Y)_N}$ and $\boldsymbol{(Y)_D}$ are related to the value for the native and denatured states, respectively. *K* values were used to calculate unfolding free energy values by $\boldsymbol{\Delta G = -RTlnK}$. With extrapolation of the linear region of $\boldsymbol{\Delta G}$ vs. denaturant concentration, the free energy for 0 M denaturant (y-intercept) was calculated as the free energy of unfolding (Pace, Grimsley, & Scholtz, 2008). The *m*-value (slope) represents the difference in the accessible surface area between the unfolded and folded state (Greene Jr & Pace, 1974; O'Brien, Brooks, & Thirumalai, 2009).

2.8. Fluorescence Quenching

Hydrogel precursor solution with 0.5 mg/mL lysozyme was aliquoted into a 96-well plate at 70 µL per well. After 45 mins of gelation, 70 µL of denaturant (GuSCN, 0–2.5 M) containing the quenching agent acrylamide (Acr, 0-200 mM) was added to each well. For ADH, after 60 min of gelation, 95 µL of denaturant (GuHCl, 0-1.5 M) containing Acr (0-200 mM) was added per well. The fluorescence intensity (Ex. 285 nm, Em. 300–400 nm, 2 nm steps) was measured in the presence of denaturant and quenching agent. Stern-Volmer plots were generated by plotting the ratio of fluorescence intensity at the maximum emission wavelength in the absence of Acr to the intensity of Acr (I_o / I) versus Acr concentration ([*Q*]). The regression slope was equated to the quenching rate (K_{sv}) according to the modified Stern-Volmer equation $I_0/I=K_{SV}[Q]+1$ (Mátyus,

Szöllősi, & Jenei, 2006). K_{SV} correlates with exposure of tryptophan to bulk solvent, implying unfolding.

2.9. Activity Assay

For lysozyme, hydrogel precursor solution with 0.5 mg/mL lysozyme was prepared and pipetted into 96-well plates at 70 µL per well. After 45 mins of gelation, 70 µL of PBS was added to the samples. The microplate was covered with TopSeal-A PLUS and the stability of lysozyme was evaluated by measuring the activity of lysozyme over 11 days in ambient conditions and in mild stressed conditions, namely 50 °C for 8 and 24 hrs, and agitation on a Sartorius CERTOMAT BS-1 orbital shaking incubator at 300 RPM and 23 °C for 1.5 and 16 days. A lysozyme activity assay was then conducted following the manufacturer's instructions. Briefly, lysozyme substrate was added to samples and controls, and the plate was mixed on an orbital shaking incubator at 37 °C and 100 RPM for 18 hrs. Fluorescence was measured at Ex/Em= 360/445 nm and 37 °C.

For ADH, hydrogel precursor solution with 0.5 mg/mL ADH was prepared and pipetted into 96-well plates at 70 µL per well. After 120 min of gelation, 70 µL of PBS or 2 M GuHCl was added to the samples to reach final concentrations of 0 (no denaturant control) or 1 M GuHCl. The microplate was covered with TopSeal-A PLUS and the stability of ADH was evaluated by measuring the activity of ADH over 6 days in ambient conditions. A mixture of 3 M ethanol and 20 mM NAD^+ dissolved in 50 mM Tris/HCl pH 8.5 and 60 µL of the mixture was added per well and mixed on an orbital shaking incubator at 23°C and 100 RPM for 10 hrs to allow for the conversion of NAD^+ to NADH. Absorption of the produced NADH was measured at 340 nm and 23 °C.

2.10. Statistical Analysis

Results are reported as mean averages with error bars of ± standard deviation of 3-6 samples from 3 independent experiments. Multiple samples were compared using single factor analysis of variance (ANOVA) followed by a Tukey's post-hoc test. A two-tailed Student's t-test was used to compare two samples. Differences between data sets were considered significant when $p < 0.05$.

3. Results

3.1. Structural Stability of Lysozyme and Alcohol Dehydrogenase Encapsulated in PEG Hydrogels

The resistance of lysozyme and ADH to chemical denaturants upon encapsulation was studied in PEG gels prepared via Michael-type addition between PEG-diSH and 4-arm PEG-Ac of varying molecular weights and PEG concentrations. (**Table 1**). The gel represented a confined environment modified by varying the molecular weight of PEG to achieve gel mesh sizes of 7.5x and 11.6x the radius of gyration of lysozyme (1.43 nm, (Krigbaum & Kuegler, 1970)) and 2.7x through 3.9x the radius of gyration of ADH (3.4 nm, (Biehl et al., 2008)). The hydrogel gelation times correlated with PEG molecular weights and PEG concentration. As a control, protein structure upon treatment with chemical denaturants was studied in a buffer (free solution, no PEG) and in un-crosslinked PEG-OH (6 kDa) solution (5% w/v in TEA buffer; crowding environment) (**Figure 1**).

3.1.1. Free Energy of Unfolding

Lysozyme, encapsulated in two PEG gels, 10/3.4 (lower mesh size, higher confinement) and 20/10 (higher mesh size, lower confinement) (**Table 1**), was exposed to 0 – 3 M GuSCN denaturant (**Figure 2A-C**). Lysozyme in PEG-OH (crowding environment) and in PBS (free solution) were used as controls. Lysozyme stability was investigated by measuring the unfolding free energy. The maximum emission wavelength (λ_{max}) is greater for proteins that are denatured

vs in their native state. **Figure S1 A** and **B** represent the λ_{max} profile and free energy, respectively, and **Figure S1 C** and **D** represent the λ_{max} profile and free energy, respectively, at an adjusted denaturant concentration. The adjusted denaturant concentration accounts for the increased GuSCN concentration "seen" by lysozyme in the PEG-OH solution and PEG gels due to excluded volume by PEG polymer chains and bound water molecules. The excluded volumes for PEG-OH, 10/3.4 gel, and 20/10 gel were estimated to be 6%, 25%, and 24% of total volume, respectively (Hoffman, 2012; Khurma & Nand, 2008; Lee, Kim, & Kim, 1997). The rest of the reported values pertain to the adjusted denaturant concentration.

When the GuSCN concentration was adjusted for excluded volume, all data points of λ_{max} had higher values in the free solution compared to other conditions (**Figure 2A**) with no significant difference in λ_{max} for lysozyme in the crowding (PEG-OH) and confined (10/3.4 gel, 20/10 gel) environments. The ΔG and *m*-value in the gels were lower compared to buffer and PEG-OH crowding solution and were lowest for the higher confinement environment (10/3.4 gel) (**Figure 2B, C**), indicating that the difference in the accessible surface area between the unfolded and folded state of lysozyme was smaller compared with lower confinement (20/10 gel), free solution (PBS buffer), and crowded (PEG-OH) environments (hence lower unfolding).

To study the effect of confinement on ADH, we chose to use different concentrations of the higher confinement 10/3.4 PEG gel, namely 5-15% w/v (**Figure 2D-F**). We again used buffer and PEG-OH crowding solutions of equivalent concentrations as controls. The rationale for using the higher confinement 10/3.4 gel only was that at the highest polymer concentration of 15% w/v, the gel mesh size of 9.2 nm (**Table 1**) approached the ADH protein diameter (4.5 nm in hydrodynamic radius and 3.4 nm in radius of gyration; (Biehl et al., 2008)). ADH was exposed to 0 – 4 M GuHCl denaturant and stability was again investigated by measuring the unfolding free energy and *m*-

value. The maximum emission wavelength (λ_{max}) for GuHCl concentrations >0.75 M was lower for hydrogels with high polymer concentration (7.5 - 15%), which provided higher confinement **(Figure 2D**). Values for free energy in buffer, 5 – 15% w/v PEG-OH (crowded environment), and 5 and 7.5% w/v PEG-hydrogel (lower confinement) were not significantly different from each other, but free energy in the 10 – 15% w/v gels was lower compared to buffer and all other conditions (**Figure 2E**). We also observed that the higher confinement provided by 7.5 - 15% (w/v) gels led to lower *m*-values for ADH compared to buffer and all other conditions with *m*-value for the 15% w/v gel being lowest from all conditions. Note that the 15% gels had a mesh size of 9.2 nm which was similar to the size of ADH. Lower *m*-values in 7.5 – 15% gels suggested the protein was significantly less denatured and less exposed to surrounding media compared with buffer, crowded environment (5 – 15 % PEG-OH), and less confined spaces (5% gel).

3.1.2. Fluorescence Quenching

The structure of PEG-encapsulated lysozyme and ADH were probed with acrylamide fluorescence quenching, which measures the degree of denaturation through the exposure of tryptophan residues to the quenching solute; a decrease in tryptophan fluorescence due to quenching is a measure of increased protein denaturation. PEG-OH (crowding) and in TEA buffer (solution) were used as controls. As expected, greater acrylamide concentrations reduced fluorescence intensity (**Figure S2A**). The normalized intensity was plotted against acrylamide concentration to obtain the Stern-Volmer constant (K_{sv}, slope of regression), which correlates to the degree of unfolding (**Figure S2B-D**). As expected, K_{sv} values in TEA buffer (solution) and PEG-OH (crowding) correlated with GuSCN concentration (**Figure 3**). Lysozyme K_{sv} values in the gels were similar for 1.5 and 2.5 M GuSCN. At 2.5 M GuSCN, K_{sv} values in the 10/3.4 and 20/10 gels (both 10% w/v) were significantly lower than in TEA buffer and PEG-OH. ADH K_{sv} values generally increased with increased in GuHCl concentration for the buffer and PEG-OH solutions.

However, K_{sv} values for ADH were not significantly different from each other as a function of denaturant concentration in the 15% w/v 10/3.4 gel, and at 1.0 M GuHCl, K_{sv} values in the 15% w/v 10/3.4 gel were significantly lower than buffer. This data suggests that in the 15% w/v gels tryptophan residues of ADH were less exposed compared to buffer, which could imply less denaturation in the presence of GuHCl. Note that only the 15% w/v 10/3.4 PEG gel was used here as it represented the highest confinement environment (see **Table 1**).

3.2. Conjugation between Lysozyme and PEG Polymers during Encapsulation

3.2.1. Conjugation of PEG with Lysozyme and ADH as Studied by PAGE

To determine whether protein-PEG conjugates form during gelation, we used two thiol crosslinkers, PEG-diSH (10 kDa polymer, 10% w/v in TEA buffer, 20 mM reactive groups) and DTT (small molecule, 0.15% w/v in TEA buffer, 20 mM reactive groups) and two unsaturated carbonyls, PEG-DA (5 kDa, 10% w/v in TEA buffer, 40 mM reactive groups), and PEG-DM (1 kDa, 10% w/v in TEA buffer, 200 mM reactive groups). Results were compared to three controls – PBS, TEA, and 10% w/v PEG-OH in TEA buffer. Lysozyme or ADH were incubated with each sample for 1 hr at ambient temperature and analyzed by SDS PAGE (**Figure 4**). Both proteins were unaffected by incubation in PEG-diSH and DTT, but a high molecular weight bands were observed in PEG-DA with lysozyme (**Figure 4A**) and PEG-DA and PEG-DM with ADH (**Figure 4B**). However, the molecular weight of these bands could not be determined due to the high concentration of unreacted PEG interfering with lane migration. However, lysozyme-PEG-DA high molecular weight species were also observed on native PAGE, where PEG does not migrate (**Figure S3**). To confirm these results were not an artifact of migration on PAGE, lysozyme was incubated in TEA buffer with PEG-DA, PEG-diSH, PEG-DM, and PEG-OH for up to 24 hrs and assayed on native PAGE (**Figure 4C** and **D**). High molecular weight species were only observed in the PEG-DA sample, and their amount increased with incubation time indicating a conjugation reaction between lysozyme and PEG-DA.

3.2.2. Conjugation between Lysozyme and PEG as Studied by High-Resolution Mass Spectrometry

To further investigate the conjugation between proteins and PEG acrylates, we chose to focus on lysozyme and conducted high-resolution mass spectrometry. Dissolved lysozyme in LC/MS grade water was used as a control and compared to lysozyme incubated (for 1 and 44 hrs) with 4-arm PEG-Ac in water at a mass ratio of 1:1 (0.5:0.5 mg/mL) and 1:20 (2:40 mg/mL) lysozyme:4-arm PEG-Ac (**Figure 5**). Results for 1 and 44 hrs were similar; for clarity only data from the 1 hr time point is shown on **Figure 5**. At the 1:1 ratio and the 1:20 ratio, approximately 6 and 115 acrylate groups per lysozyme, respectively, existed. At the lower 4-arm PEG-Ac concentration (1:1 ratio), we observed unbound lysozyme and potentially conjugates of lysozyme with 4-arm PEG-Ac after 1 and 44 hrs. The mass spectrum of the lysozyme:4-arm PEG-Ac mass ratio of 1:1 sample (**Figure 5A**) indicates the presence of unbound lysozyme by distinct peaks at 1800 and 2000 m/z (with +8 and +7 charges, respectively). However, the mass spectrum for the 1:20 mass ratio sample lacked such distinct peaks (**Figure 5B**), indicating no unbound lysozyme. Our results indicate that within 1 hr, all lysozyme formed conjugates in the 1:20 samples, but some lysozyme remained unconjugated in the 1:1 samples. Note that after conjugation to excess 4-arm PEG-Ac, lysozyme activity was maintained at a comparable level to that of unconjugated lysozyme (**Figure S4**).

To identify the fragments of lysozyme that conjugate with the acrylate group in 4-arm PEG-Ac, stock solutions were digested with trypsin, which cleaves peptide bonds at the carboxyl side of arginine and lysine residues (Olsen, Ong, & Mann, 2004). Total ion chromatograms (**Figure 6**) of lysozyme incubated with 4-arm PEG-Ac showed distinct peaks around 7 – 9 and 13 – 15 mins that were not present in the control samples of lysozyme alone; these peaks indicated the presence of lysozyme fragments that were conjugated with 4-arm PEG-Ac. Further analysis of

the lysozyme fragments using mass spectrometry (4 MS/MS scans for each run) suggested that 4-arm PEG-Ac conjugated with lysozyme residue(s) 71 – 81 (**Figure S5**).

3.2.3. Conjugation between Lysozyme and PEG as Studied by Rheology

We further used rheology to determine the conjugation of lysozyme to 4-arm PEG-Ac as a function of time. Lysozyme was incubated with 4-arm PEG-Ac for up to 24 hrs prior to adding PEG-diSH crosslinker, and *G'* was monitored during gelation **(Figure 7**). At 50 min, lower values of *G'* for the gel samples formed from lysozyme incubated with 4-arm PEG-Ac for 24 hr vs 1 hr and 3 hr (**Figure 7A**) suggested that the lysozyme - 4-arm PEG-Ac conjugates continued to form for up to at least 1 day. The changes in gelation time (**Figure 7B**) for the control (no lysozyme) vs 0, and 1 hr of incubation prior to gelation were statistically similar. These results indicate that lysozyme was not reacting with 4-arm PEG-Ac during hydrogel formation for up to 1 hr.

3.3. Enzymatic Activity of Encapsulated Protein

The activity of lysozyme embedded in PBS buffer, PEG-OH, 10/3.4 gel, and 20/10 gel was monitored at room temperature for 11 days, during which time, no significant changes in lysozyme activity were observed (**Figure 8A**). Additionally, mild stress conditions, 50°C (heat) or shaking at 300 RPM (mechanical agitation) were examined. All samples retained >80% activity when incubated at 50°C for up to 24 hrs or agitated for up to 16 days.

Similarly, the activity of ADH dissolved in buffer or 5, 10, and 15% w/v PEG-OH and encapsulated in a 5, 10, or 15% w/v 10/3.4 gel was monitored at room temperature for 6 days (**Figure 10**). Overall, the activity did not decline over 6 days when no denaturant was added. Where we had 1 M denaturant, activity appeared to be highest in the gel samples and lowest in buffer compared with the other conditions at day 2 and 6. Between 0-2 days, ADH activity decreased by ~92% in buffer, ~76-82% in PEG-OH and ~67-77% in the gels. Between 2-6 days, ADH activity decreased

by ~87% in buffer, ~68-89% in PEG-OH and ~73-85% in the gels. Further, on day 2 activity in the 10 and 15% gel was significantly higher than the 10 and 15% PEG-OH. On day 6 in the presence of GuHCl, 10 and 15% w/v PEG-OH and gel showed higher activity than 5% w/v PEG-OH and gel, respectively. Our results indicate that the higher concentration PEG solutions and gels had mildly protective effects on enzyme activity upon exposure to GuHCl when compared to buffer.

4. Discussion

4.1. Strengths and Limitations of the Experimental Model

Here, we tested the effect of encapsulation and confinement in PEG hydrogels on lysozyme and ADH stability and activity under stress conditions meant to induce denaturation. Lysozyme and ADH were chosen as model proteins because the activity of each can be easily measured, and they have multiple tryptophan residues which allow for robust intrinsic fluorescence measurements. However, their different sizes (Lysozyme -14.3 kDa, ADH (tetramer) – 147 kDa) allowed us to probe the effect of confinement, specifically gel mesh size relative to protein diameter. To delineate the effect of confinement in the PEG gels, we used two control conditions: protein in a free solution (PBS or TEA buffer) and protein in a PEG-OH solution, where PEG-OH was a crowding environment and allowed us to probe for interactions between the protein and the PEG backbone. For direct comparison of results, we adjusted the denaturant concentrations (GuSCN and GuHCl) and acrylamide to account for excluded volume by the PEG polymer and its layers of bound water. Likewise, convective and diffusive mass transfer should be reduced in a hydrogel compared to the crowding and free solutions, possibly slowing down dispersal of solutes. It was estimated that guanidinium would diffuse through the gel in 100 min, assuming 1D Fickian diffusion though a 2.2 mm thick gel, a diffusivity of 6.5×10^{-6} cm^2/sec in water, and reduction in effective diffusivity of 40% in the hydrogel (Gannon, Larsson, Greer, & Thompson, 2008; Silviya P Zustiak, Boukari, & Leach, 2010). However, the tertiary structure of lysozyme responds rapidly to changes in denaturant concentration (van den Berg, Ellis, & Dobson, 1999), and we suggest

that differences in exposure time had minimal impact on lysozyme unfolding as the experiment was conducted for 120 min while it should have taken ~100 min for an equilibrium concentration of GuSCN or acrylamide to be reached between the surrounding solution and the gel.

4.2. PEG Hydrogels Reduced Unfolding of Lysozyme and ADH at High Denaturant Concentrations

Others have shown that crowding and confinement could preserve protein structure, stability, and activity (Eggers & Valentine, 2001; Ghosh et al., 2020; Wang & Akcora, 2017) but few have focused on PEG gels (Simpson et al., 2020). Our data indicated that PEG gels did not destabilize lysozyme, although no clear conclusion could be drawn whether lysozyme was stabilized. The free energy of unfolding (**Figure 2A-C**) did not significantly differ between the free solution (PBS), crowding and confinement for the range of denaturant concentrations explored. However, ADH was observed to be more stable by free energy of unfolding (**Figure 2D-F**) as the extent of confinement increased with increasing PEG concentration in the gels. Intrinsic fluorescence and fluorescence quenching measurements (**Figure 3**) revealed both crowding and confinement reduced the accessible surface area of both proteins compared to free solution at high denaturant concentrations. While the confining environment did not stabilize lysozyme, lower accessible surface area corresponds to a less unfolded structure.

Note that the gels had mesh sizes ~7.5x and 11.6x the radius of gyration of lysozyme and 2.7x – 3.9x the radius of gyration of ADH. Thermodynamic modeling suggests the stabilizing effect of confinement becomes more pronounced as dimensions of the confining environment approach the protein diameter (Hayer-Hartl & Minton, 2006; Wang & Akcora, 2017). The free energy of unfolding of ADH was significantly reduced in 10% w/v 10/3.4 gel, corresponding to a mesh size of 10.7 nm or 3.1x the radius, and the effect became more pronounced in higher concentration gels with tighter mesh (**Figure 2D-F)**. Unfolded protein has less entropy and fewer conformations

in confinement as it has in free solution, where it can easily form any conformation (Rathore, Knotts IV, & de Pablo, 2006; Zhou, 2008). However, conformational changes can occur without loss of enzymatic activity or efficacy. In our study, both lysozyme and ADH maintained their enzymatic activity within the confining environment, and ADH retained higher activity in the gels compared to free solution in the presence of denaturant (**Figure 8, Figure 9**). This stabilization was potentially due to a change in the entropy of unfolding. The unfolded protein is less favorable in a confined space compared with in free solution due to excluded volume and spatial barriers.

4.3. Proteins Become PEGylated in the Presence of Michael-Type Addition Chemistries

The PEG gel used here was made via Michael-type addition between a multi-arm PEG-acrylate monomer and a PEG-dithiol crosslinker. The reaction occurs under physiological conditions and is highly specific, suitable for protein encapsulation. We have previously shown that proteins can be encapsulated in similar PEG hydrogels without causing structural changes or aggregation (Silviya P. Zustiak & Leach, 2010, 2011). Contrarily, others have shown that proteins might interact with functionalized PEG during gelation via nucleophilic reactions with α,β-unsaturated carbonyl compounds, disruption of disulfide bridges from thiol-functionalized polymers, or hydrophobic interactions (Hammer, Brandl, Kirchhof, Messmann, & Goepferich, 2015; Paidikondala, Wang, Hilborn, Larsson, & Varghese, 2019). Note that lysozyme has four disulfide bonds and a relatively hydrophobic surface and may be susceptible to such interactions. However, the PEG gels used here form a gel at ambient temperature in less than 1 hr (**Table 1**), hence we hypothesized that conjugation would not be a major concern in that time frame.

To test this hypothesis, lysozyme and ADH were combined with PEG-DA and PEG-DM and analyzed by PAGE. Both exhibited high molecular weight bands after one hour of incubation by SDS-PAGE. Lysozyme was further incubated for up to 24 hours, and high molecular weight

species continued to form throughout the incubation (**Figure 4C**). Mass spectroscopy confirmed PEG-lysozyme conjugate formed rapidly in a molar excess of acrylate reactive groups (1:20 ratio) (**Figure 5**), and lysozyme digestion analysis suggested the conjugation occurred on lysozyme segment 71 – 81, which contains a lysine residue. Note that in the absence of thiols, the primary amines of lysine and arginine can also react with acrylates through the same mechanism as thiols, albeit at a slower rate (Mather, Viswanathan, Miller, & Long, 2006). We suggest that acrylate reaction with thiols would dominate in the short time frame required for PEG gelation (<1 hr), but reaction with amines might become dominant at later time points due to their relative abundance compared to free thiols. To form the gels here, acrylates and thiols were added in a 1:1 stoichiometric ratio, resulting in two competing reactions – 4-arm PEG-Ac and PEG-diSH crosslinking to form the gel, and 4-arm PEG-Ac and the encapsulated protein to form a PEGylated conjugate. Since the Ac/SH reaction has a faster reaction rate it is expected to consume the majority of the acrylate groups (Mather et al., 2006).

5. Conclusions

In this study we compared the structure of two model proteins, lysozyme and ADH, encapsulated in a confining PEG gel, a crowding PEG solution, and a free buffer. Although lysozyme exhibited no significant difference in free energy of unfolding, encapsulated lysozyme had less exposed surface area in its unfolded state, indicating that confinement did not preserve the native conformation but prevented complete unfolding. ADH was significantly stabilized as measured by free energy of unfolding as the mesh size of the gel approached its radius of gyration. Lysozyme enzymatic activity was equally retained across the free, crowding, and confining environments when exposed to mild stress conditions. ADH enzymatic activity was better retained in the crowded environment and the gel compared to buffer when exposed to GuHCl. Lastly, we demonstrated that lysozyme and ADH may conjugate with PEG-acrylate at long reaction times. These proteins were used as models for therapeutic proteins to provide a deeper understanding

of the impact of hydrogel encapsulation on conformational stability, which will provide for rationally designed technologies for the improved formulation, storage and delivery of protein therapeutics.

Acknowledgements

JL funding: National Institutes of Health (5R01GM117159). We thank Samuel Stealey (SLU) for support with rheology. We thank Dr. Theresa Good (National Science Foundation) for insightful discussions about protein structure and function. We thank Dr. Zeev Rosenzweig and Laura Kesner (Chemistry, UMBC) for access to the Spectra Max M5. We thank Joshua Wilhide in the Molecular Characterization and Analysis Complex at UMBC for technical support.

References

Asuri, P., & Kunkel, J. (2014). Function, Structure, and Stability of Enzymes Confined in Agarose Gels. *Plos One, 9*(1). doi:ARTN e86785

10.1371/journal.pone.0086785

Bhattarai, N., Ramay, H. R., Gunn, J., Matsen, F. A., & Zhang, M. (2005). PEG-grafted chitosan as an injectable thermosensitive hydrogel for sustained protein release. *Journal of Controlled Release, 103*(3), 609-624.

Biehl, R., Hoffmann, B., Monkenbusch, M., Falus, P., Préost, S., Merkel, R., & Richter, D. (2008). Direct observation of correlated interdomain motion in alcohol dehydrogenase. *Physical review letters, 101*(13), 138102.

Bolis, D., Politou, A. S., Kelly, G., Pastore, A., & Temussi, P. A. (2004). Protein stability in nanocages: a novel approach for influencing protein stability by molecular confinement. *Journal of Molecular Biology, 336*(1), 203-212.

Bryant, S. J., Bender, R. J., Durand, K. L., & Anseth, K. S. (2004). Encapsulating chondrocytes in degrading PEG hydrogels with high modulus: engineering gel structural changes to facilitate cartilaginous tissue production. *Biotechnology and bioengineering, 86*(7), 747-755.

Calvet, D., Wong, J. Y., & Giasson, S. (2004). Rheological Monitoring of Polyacrylamide Gelation: Importance of Cross-Link Density and Temperature. *Macromolecules, 37*(20), 7762-7771. doi:10.1021/ma049072r

Cheng, K., Wu, Q., Zhang, Z., Pielak, G. J., Liu, M., & Li, C. (2018). Crowding and Confinement Can Oppositely Affect Protein Stability. *ChemPhysChem, 19*(24), 3350-3355. doi:10.1002/cphc.201800857

Chu, X., Suo, Z., & Wang, J. (2020). Confinement and Crowding Effects on Folding of a Multidomain Y-Family DNA Polymerase. *Journal of Chemical Theory and Computation, 16*(2), 1319-1332.

Eggers, D. K., & Valentine, J. S. (2001). Molecular confinement influences protein structure and enhances thermal protein stability. *Protein Science, 10*(2), 250-261. doi:10.1110/ps.36201

Gannon, G., Larsson, J. A., Greer, J. C., & Thompson, D. (2008). Guanidinium chloride molecular diffusion in aqueous and mixed water-ethanol solutions. *J Phys Chem B, 112*(30), 8906-8911. doi:10.1021/jp8030336

Ghosh, S., Shahid, S., Raina, N., Ahmad, F., Hassan, M. I., & Islam, A. (2020). Molecular and macromolecular crowding-induced stabilization of proteins: Effect of dextran and its building block alone and their mixtures on stability and structure of lysozyme. *International Journal of Biological Macromolecules, 150*, 1238-1248. doi:https://doi.org/10.1016/j.ijbiomac.2019.10.135

Greene Jr, R. F., & Pace, C. N. (1974). Urea and Guanidine Hydrochloride Denaturation of Ribonuclease, Lysozyme, α-Chymotrypsin, and b-Lactoglobulin. *Journal of Biological Chemistry, 249*(17), 5388-5393.

Hammer, N., Brandl, F. P., Kirchhof, S., Messmann, V., & Goepferich, A. M. (2015). Protein compatibility of selected cross-linking reactions for hydrogels. *Macromolecular Bioscience, 15*(3), 405-413.

Hayer-Hartl, M., & Minton, A. P. (2006). A simple semiempirical model for the effect of molecular confinement upon the rate of protein folding. *Biochemistry, 45*(44), 13356-13360.

Hoffman, A. S. (2012). Hydrogels for biomedical applications. *Advanced drug delivery reviews, 64*, 18-23.

Jain, E., Flanagan, M., Sheth, S., Patel, S., Gan, Q., Patel, B., . . . Zustiak, S. P. (2020). Biodegradable polyethylene glycol hydrogels for sustained release and enhanced stability of rhGALNS enzyme. *Drug delivery and translational research, 10*(5), 1341-1352.

Jain, E., Sheth, S., Dunn, A., Zustiak, S. P., & Sell, S. A. (2017). Sustained release of multicomponent platelet-rich plasma proteins from hydrolytically degradable PEG hydrogels. *Journal of Biomedical Materials Research Part A, 105*(12), 3304-3314. doi:10.1002/jbm.a.36187

Kharkar, P. M., Kloxin, A. M., & Kiick, K. L. (2014). Dually degradable click hydrogels for controlled degradation and protein release. *Journal of materials chemistry. B, 2*(34), 5511-5521. doi:10.1039/c4tb00496e

Khurma, J. R., & Nand, A. V. (2008). Temperature and pH sensitive hydrogels composed of chitosan and poly(ethylene glycol). *Polymer Bulletin, 59*(6), 805-812. doi:10.1007/s00289-007-0817-2

Krigbaum, W. R., & Kuegler, F. R. (1970). Molecular conformation of egg-white lysozyme and bovine α-lactalbumin in solution. *Biochemistry, 9*(5), 1216-1223. doi:10.1021/bi00807a024

Lee, Y. M., Kim, S. S., & Kim, S. H. (1997). Synthesis and properties of poly(ethylene glycol) macromer/β-chitosan hydrogels. *Journal of Materials Science: Materials in Medicine, 8*(9), 537-541. doi:10.1023/A:1018594614087

Li, J., & Mooney, D. J. (2016). Designing hydrogels for controlled drug delivery. *Nature reviews. Materials, 1*(12), 16071. doi:10.1038/natrevmats.2016.71

Lin, C.-C., & Anseth, K. S. (2009). PEG hydrogels for the controlled release of biomolecules in regenerative medicine. *Pharmaceutical research, 26*(3), 631-643.

Lutolf, M. P., Lauer-Fields, J. L., Schmoekel, H. G., Metters, A. T., Weber, F. E., Fields, G. B., & Hubbell, J. A. (2003). Synthetic matrix metalloproteinase-sensitive hydrogels for the conduction of tissue regeneration: engineering cell-invasion characteristics. *Proceedings of the National Academy of Sciences, 100*(9), 5413-5418.

Mather, B. D., Viswanathan, K., Miller, K. M., & Long, T. E. (2006). Michael addition reactions in macromolecular design for emerging technologies. *Progress in Polymer Science, 31*(5), 487-531. doi:https://doi.org/10.1016/j.progpolymsci.2006.03.001

Mátyus, L., Szöllősi, J., & Jenei, A. (2006). Steady-state fluorescence quenching applications for studying protein structure and dynamics. *Journal of Photochemistry and Photobiology B: Biology, 83*(3), 223-236. doi:https://doi.org/10.1016/j.jphotobiol.2005.12.017

Minton, A. P. (1992). Confinement as a determinant of macromolecular structure and reactivity. *Biophysical Journal, 63*(4), 1090-1100.

Minton, A. P. (2006). How can biochemical reactions within cells differ from those in test tubes? *Journal of cell science, 119*(14), 2863-2869.

Nair, D. P., Podgórski, M., Chatani, S., Gong, T., Xi, W., Fenoli, C. R., & Bowman, C. N. (2014). The Thiol-Michael Addition Click Reaction: A Powerful and Widely Used Tool in Materials Chemistry. *Chemistry of Materials, 26*(1), 724-744. doi:10.1021/cm402180t

Nakano, S.-i., Yamaguchi, D., & Sugimoto, N. (2018). Thermal stability and conformation of DNA and proteins under the confined condition in the matrix of hydrogels. *Molecular Biology Reports*(4), 403. doi:10.1007/s11033-018-4174-z

Natarajan, A., Xiong, C. Y., Albrecht, H., DeNardo, G. L., & DeNardo, S. J. (2005). Characterization of site-specific ScFv PEGylation for tumor-targeting pharmaceuticals. *Bioconjug Chem, 16*(1), 113-121. doi:10.1021/bc0498121

O'Brien, E. P., Brooks, B. R., & Thirumalai, D. (2009). Molecular origin of constant m-values, denatured state collapse, and residue-dependent transition midpoints in globular proteins. *Biochemistry, 48*(17), 3743-3754. doi:10.1021/bi8021119

Olsen, J. V., Ong, S.-E., & Mann, M. (2004). Trypsin cleaves exclusively C-terminal to arginine and lysine residues. *Molecular & Cellular Proteomics, 3*(6), 608-614.

Pace, C. N., Grimsley, G. R., & Scholtz, J. M. (2008). Denaturation of proteins by urea and guanidine hydrochloride. *Protein Science Encyclopedia: online*, 45-69.

Pace, C. N., & Shaw, K. L. (2000). Linear extrapolation method of analyzing solvent denaturation curves. *Proteins: Structure, Function, and Bioinformatics, 41*(S4), 1-7.

Paidikondala, M., Wang, S., Hilborn, J. n., Larsson, S., & Varghese, O. P. (2019). Impact of Hydrogel Cross-Linking Chemistry on the in Vitro and in Vivo Bioactivity of Recombinant Human Bone Morphogenetic Protein-2. *ACS Applied Bio Materials, 2*(5), 2006-2012.

Rathore, N., Knotts IV, T. A., & de Pablo, J. J. (2006). Confinement effects on the thermodynamics of protein folding: Monte Carlo simulations. *Biophysical Journal, 90*(5), 1767-1773.

Rosenberg, A. S. (2006). Effects of protein aggregates: an immunologic perspective. *The AAPS journal, 8*(3), E501-E507. doi:10.1208/aapsj080359

Simpson, L. W., Szeto, G. L., Boukari, H., Good, T. A., & Leach, J. B. (2020). Impact of four common hydrogels on amyloid-β (Aβ) aggregation and cytotoxicity: Implications for 3D models of Alzheimer's disease. *ACS omega, 5*(32), 20250-20260.

Van de Wetering, P., Metters, A. T., Schoenmakers, R. G., & Hubbell, J. A. (2005). Poly (ethylene glycol) hydrogels formed by conjugate addition with controllable swelling, degradation, and release of pharmaceutically active proteins. *Journal of Controlled Release, 102*(3), 619-627.

van den Berg, B., Ellis, R. J., & Dobson, C. M. (1999). Effects of macromolecular crowding on protein folding and aggregation. *The EMBO journal, 18*(24), 6927-6933.

Wang, H., & Akcora, P. (2017). Confinement effect on the structure and elasticity of proteins interfacing polymers. *Soft Matter, 13*(8), 1561-1568.

Xu, G., Cheng, K., Wu, Q., Liu, M., & Li, C. (2017). Confinement alters the structure and function of calmodulin. *Angewandte Chemie, 129*(2), 545-549.

Zhou, H.-X. (2008). Protein folding in confined and crowded environments. *Archives of biochemistry and biophysics, 469*(1), 76-82. doi:10.1016/j.abb.2007.07.013

Zhou, H.-X., Rivas, G., & Minton, A. P. (2008). Macromolecular crowding and confinement: biochemical, biophysical, and potential physiological consequences. *Annu. Rev. Biophys., 37*, 375-397.

Zustiak, S. P., Boukari, H., & Leach, J. B. (2010). Solute diffusion and interactions in cross-linked poly (ethylene glycol) hydrogels studied by fluorescence correlation spectroscopy. *Soft Matter, 6*(15), 3609-3618.

Zustiak, S. P., & Leach, J. B. (2010). Hydrolytically Degradable Poly(Ethylene Glycol) Hydrogel Scaffolds with Tunable Degradation and Mechanical Properties. *Biomacromolecules, 11*(5), 1348-1357. doi:10.1021/bm100137q

Zustiak, S. P., & Leach, J. B. (2011). Characterization of protein release from hydrolytically degradable poly(ethylene glycol) hydrogels. *Biotechnology and Bioengineering, 108*(1), 197-206. doi:10.1002/bit.22911

Table 1: Properties of PEG hydrogels formed from varying PEG concentration and molecular weight PEG-diSH and 4-arm PEG-Ac.

Gel Types	$MW_{4\text{-arm PEG-Ac}}$ (kDa)	$MW_{PEG\text{-diSH}}$ (kDa)	[PEG] (%w/v)	[Ac] (mM)	[SH] (mM)	[Lyso] (nM)	[ADH] (nM)	Gelation Time (min)	Mesh Size (nm)
20/10 gel	20	10	10	10.0	10.0	350	N/A	46.3 ± 2.0	16.6 ± 1.0
10/3.4 gel	10	3.4	5	11.9	11.9	N/A	3.5	44.1 ± 0.9	13.3 ± 0.1
			7.5	17.9	17.9	N/A	3.5	38.5 ± 0.3	11.8 ± 0.2
			10	23.8	23.8	350	3.5	34.1 ± 0.4	10.7 ± 0.3
			12.5	29.8	29.8	N/A	3.5	25.6 ± 1.7	10.1 ± 0.2
			15	37.5	37.5	N/A	3.5	19.6 ± 0.5	9.2 ± 0.1

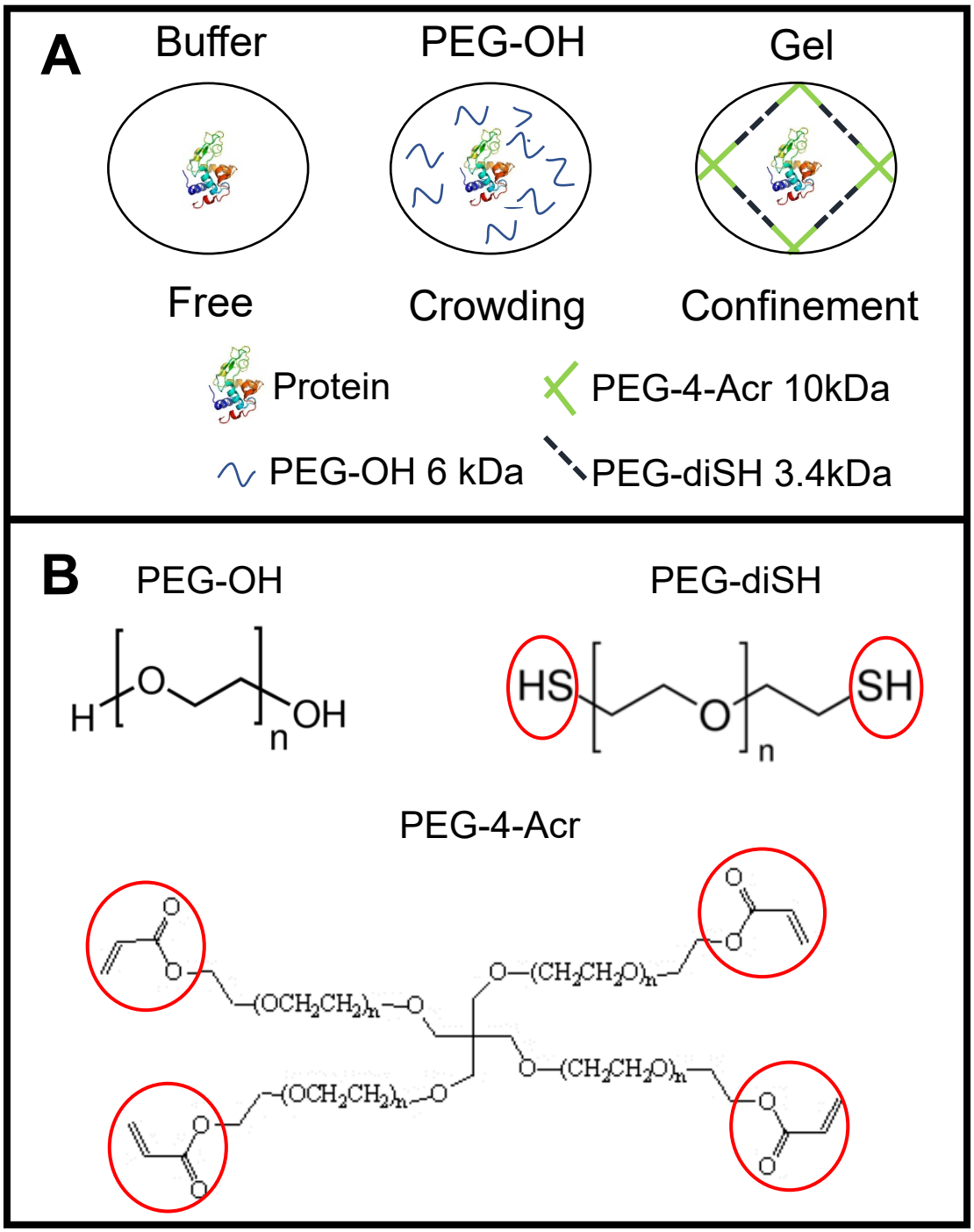

Figure 1: Schematic representation of experimental conditions. A) Schematic representation of the three experimental, namely free solution, crowding and confinement. **B)** Chemical structures of polyethylene glycol (PEG) polymers. Red circles indicate the reactive groups used in Michael-Type addition gelation reaction.

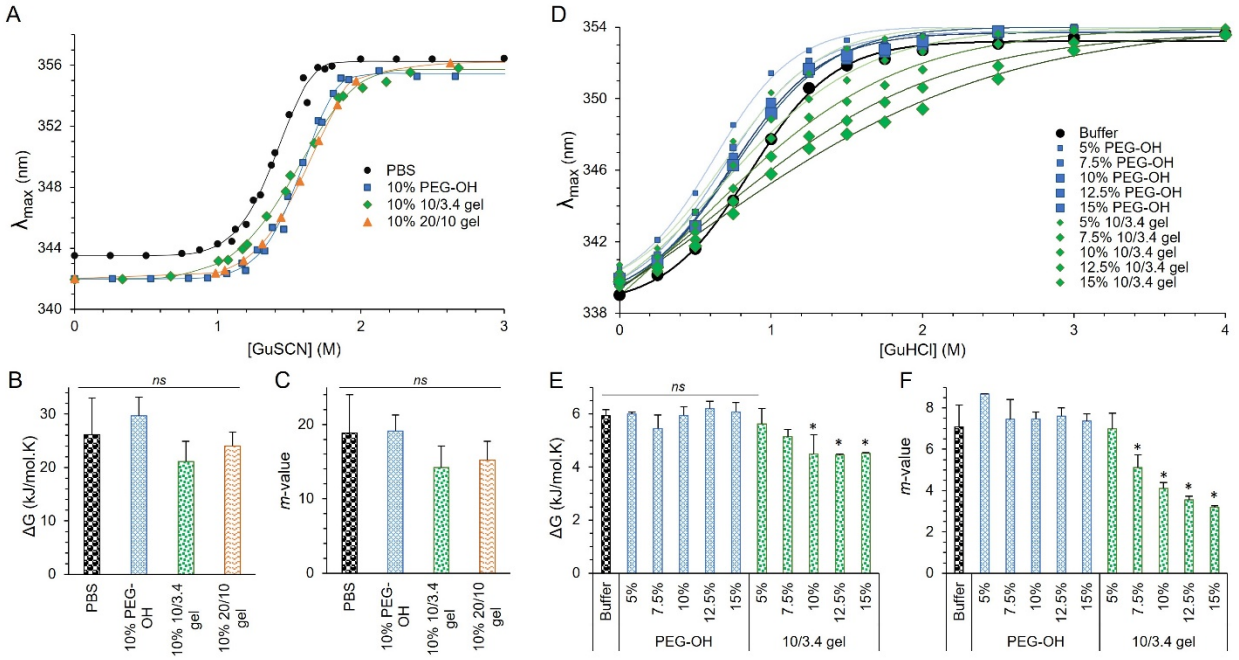

Figure 2: Free energy of unfolding for lysozyme and ADH in different environments upon exposure to denaturant. A) Maximum emission intensity wavelength, Ex: 295 nm and Em: 300—400 nm, **B)** free energy, and **C)** *m*-value for lysozyme (0.25 mg/mL) in buffer (PBS, free solution), PEG-OH (crowding), 10/3.4 gel and 20/10 gel (confinement) at various denaturant concentrations. **D)** Maximum emission intensity wavelength, Ex: 295 nm and Em: 300—400 nm, **E)** free energy, and **F)** *m*-value for alcohol dehydrogenase (~0.25 mg/mL) in buffer (free solution), PEG-OH (crowding), 10/3.4 gel (confinement) at various denaturant concentrations (n=3). Statistical significance denoted by * ($p < 0.05$, $n = 3$).

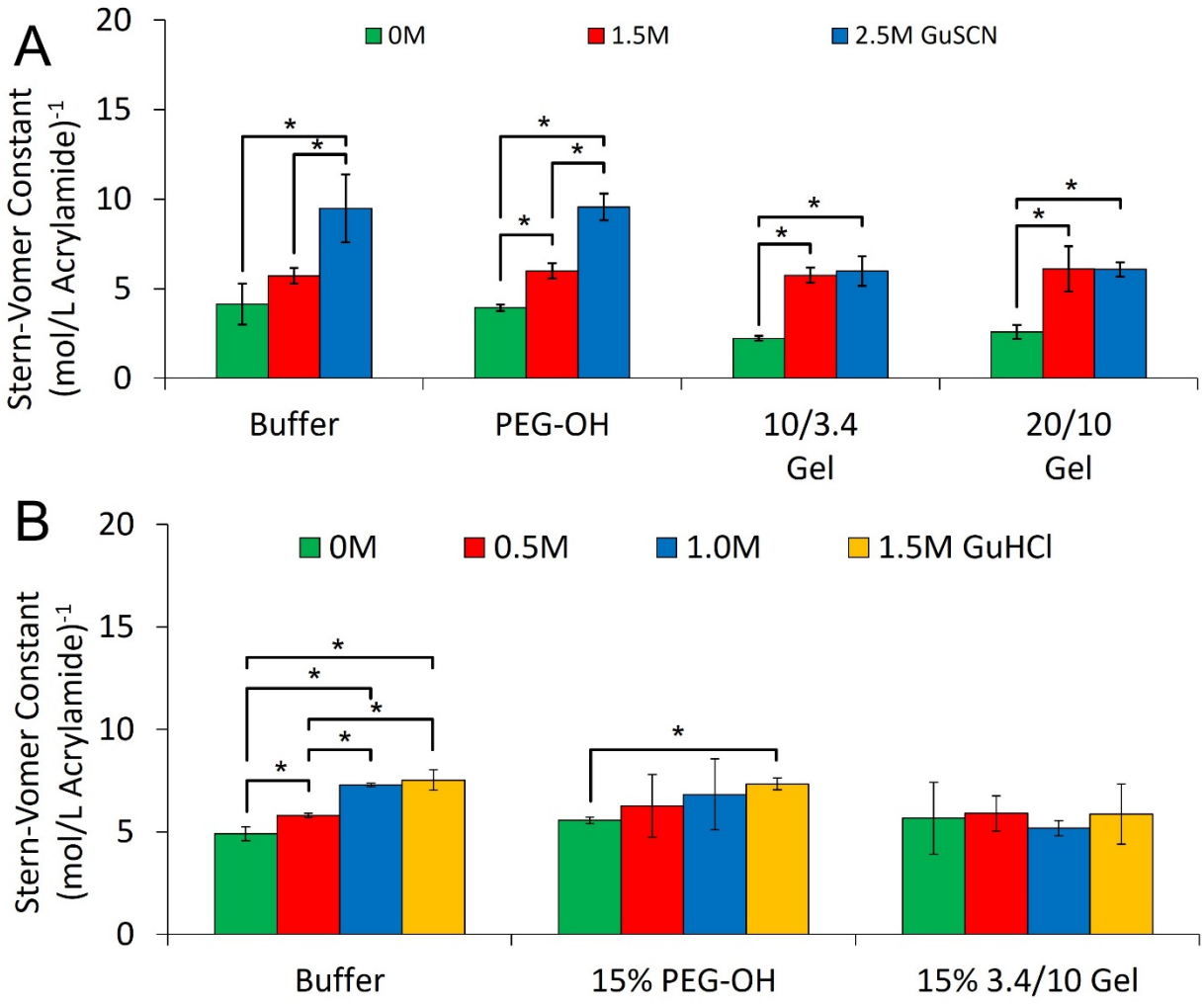

Figure 3: Acrylamide fluorescence quenching for lysozyme and ADH in different environments upon exposure to denaturant. A) Stern-Volmer constants of 0.25mg/mL lysozyme in TEA buffer (free solution), PEG-OH (crowding), 10% w/v 10/3.4 gel and 10% w/v 20/10 gel (confinement) at three denaturant concentrations. **B)** Stern-Vomer constants of 0.21 mg/mL ADH in TEA buffer (free solution) and 15% w/v 10/3.4 gel. Stern-Volmer constants were adjusted for the excluded volume increasing the local concentration of acrylamide. Statistical significance denoted by * ($p < 0.05$, n = 3).

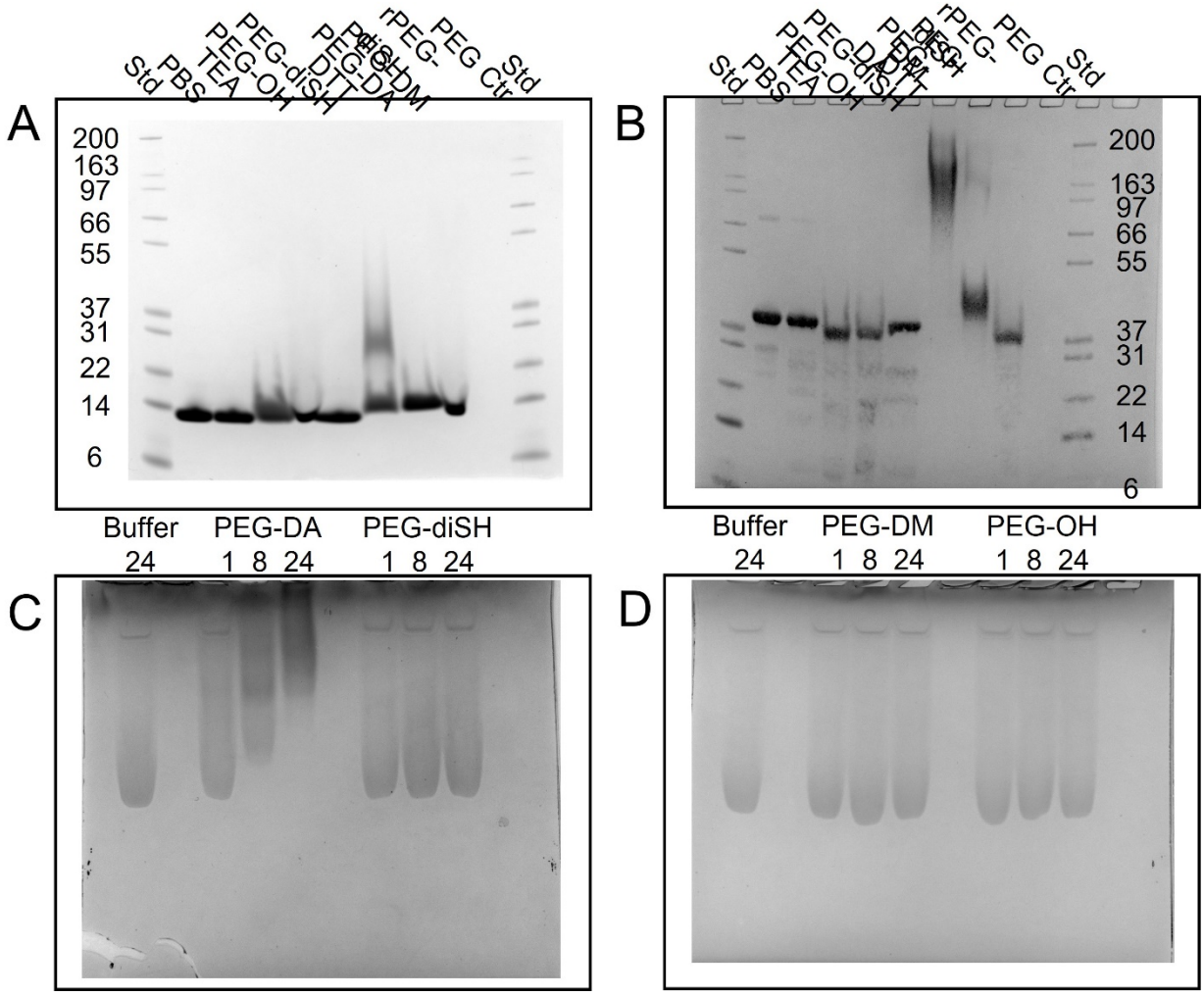

Figure 4: Non-reduced SDS and Native PAGE for lysozyme and ADH incubated with different buffers and PEG polymers with various reactive groups. A) SDS-PAGE of lysozyme (0.5 mg/mL) after 1 hr incubation with various PEG polymer (10% w/v) or DTT (0.15% w/v). All samples were run non-reduced with the exception of rPEG-diSH. PEG-Ctr indicates PEG-OH without lysozyme. **B)** SDS-PAGE of ADH as in A. **C)** Native PAGE of lysozyme (0.5mg/mL) after incubation with PEG-DA or PEG-diSH (10% w/v) for 1, 8, and 24 hours. **D)** Native PAGE of lysozyme (0.5 mg/mL) after incubation with PEG-DM or PEG-OH (10% w/v) for 1, 8, and 24 hours. All incubations were performed at ambient temperature.

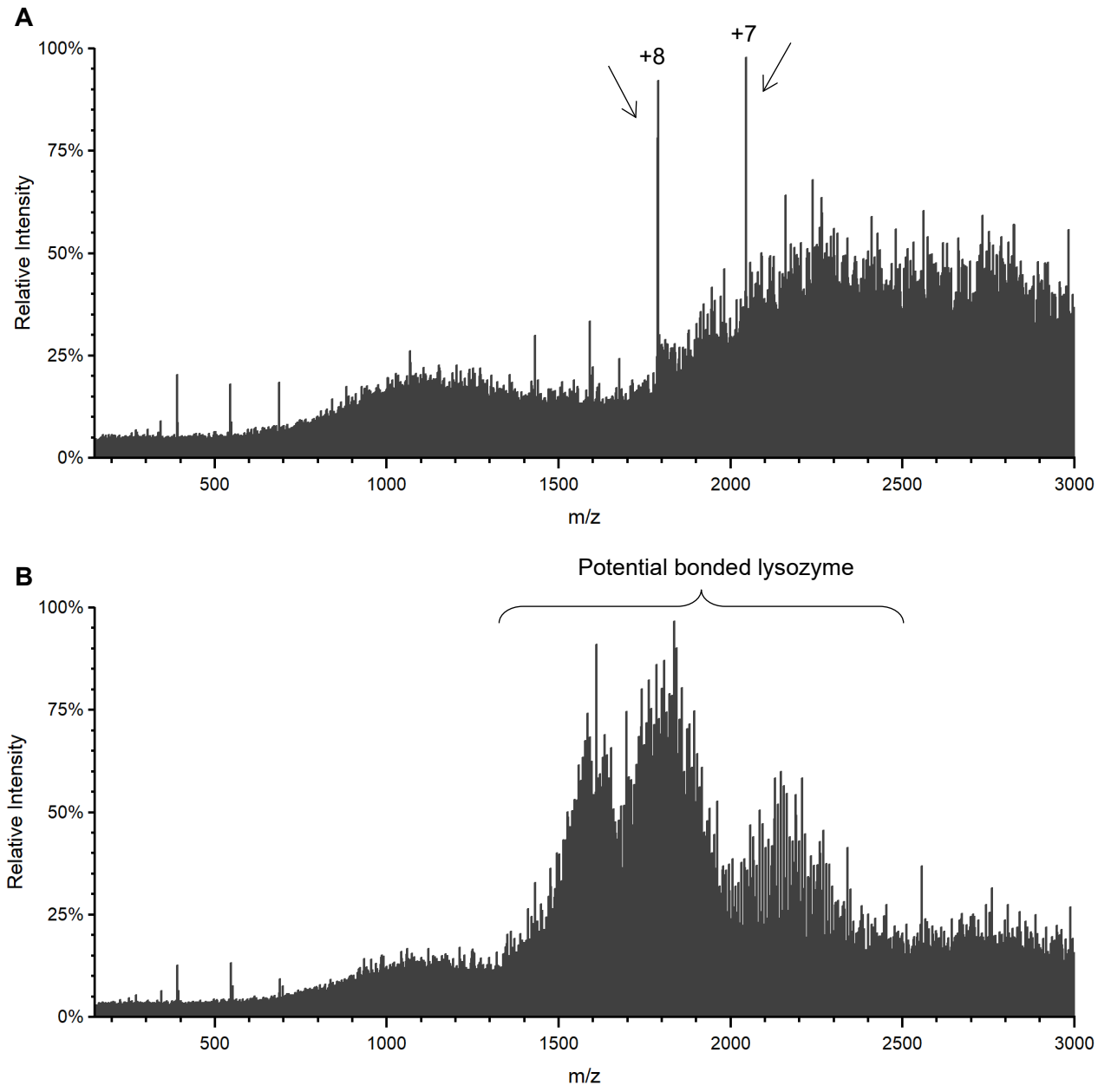

Figure 5: High-resolution mass spectrometry for lysozyme incubated with 4-arm PEG-Ac for 1 hour. A) 1:1 ratio of lysozyme to 4-arm PEG-Ac 10 kDa in water. **B)** 1:20 ratio of lysozyme to 4-arm PEG-Ac 10 kDa in water.

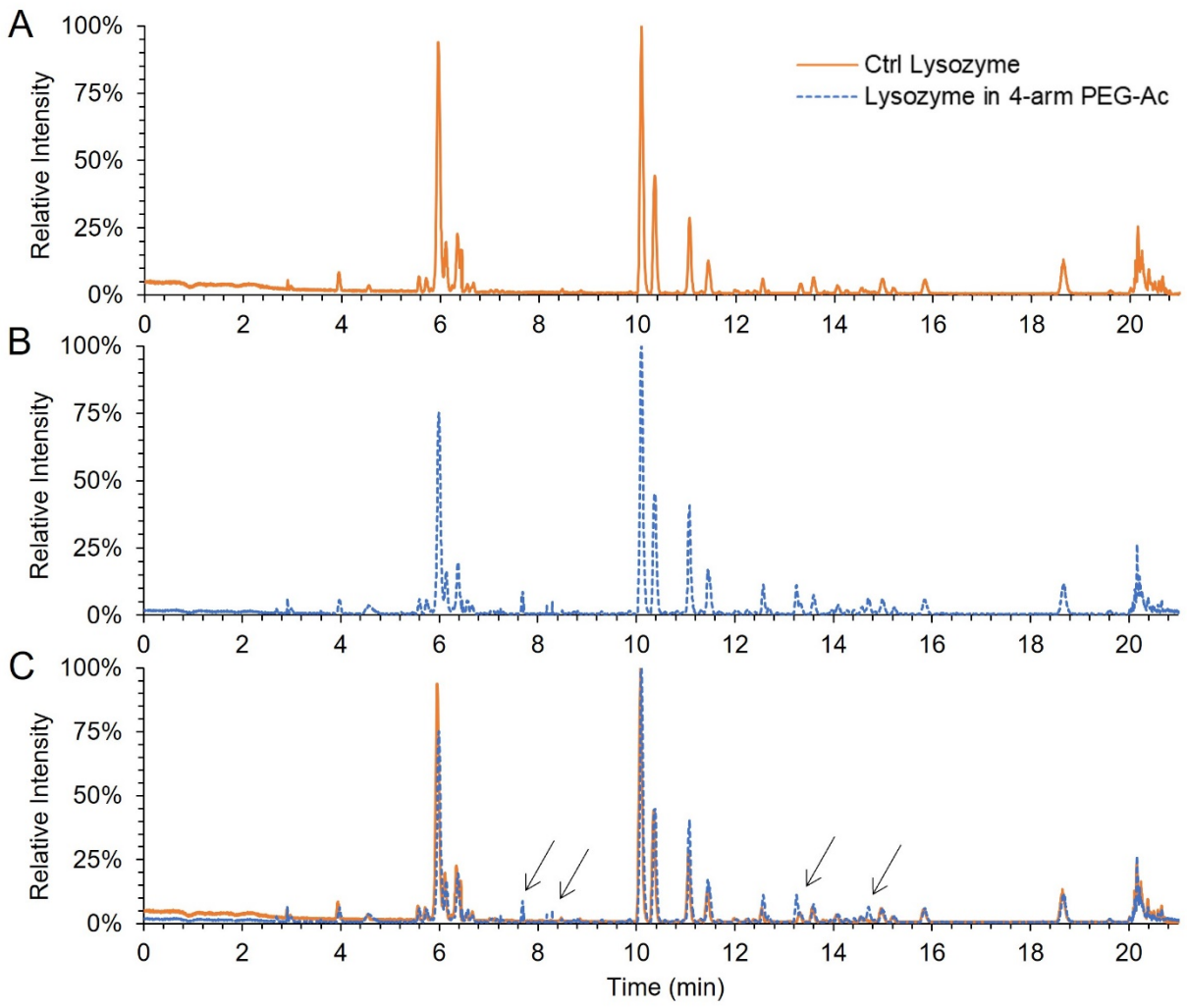

Figure 6: Total ion chromatograms of trypsin-digested lysozyme. A) Control lysozyme. **B)** Lysozyme incubated with 4-arm PEG-Ac at 1:20 mass ratio for 1 hour. **C)** Overlap of A and B.

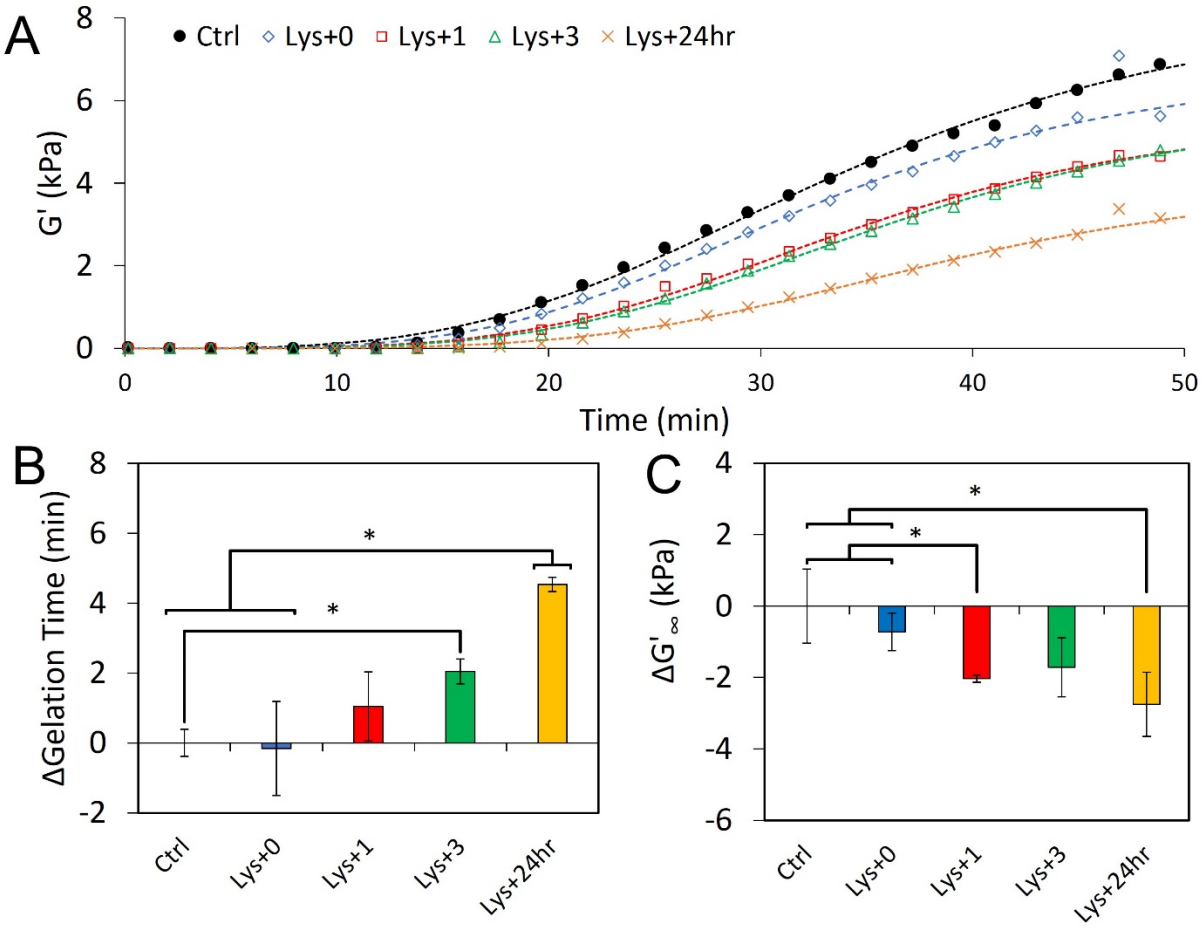

Figure 7: Hydrogel stiffness and gelation time as a function of pre-incubation of lysozyme with 4-arm PEG-Ac. A) Increase gel storage modulus, *G'*, over time during gelation. Ctrl refers to PEG (10% w/v) hydrogel without lysozyme. For all other conditions, lysozyme was pre-incubated with 4-arm PEG-Ac for 0 (Lys+0), 1 (Lys+1), 3 (Lys+3), and 24 (Lys+24) hours prior to gel formation. Lines are provided to guide the eye. **B)** Change in gelation time as a function of lysozyme-4-arm PEG-Ac incubation, where gelation time was defined as time required to reach half of maximum *G'*. **C)** Change in *G'* as a function of lysozyme-4-arm PEG-Ac incubation. Statistical significance denoted by * ($p < 0.05$, $n = 3$).

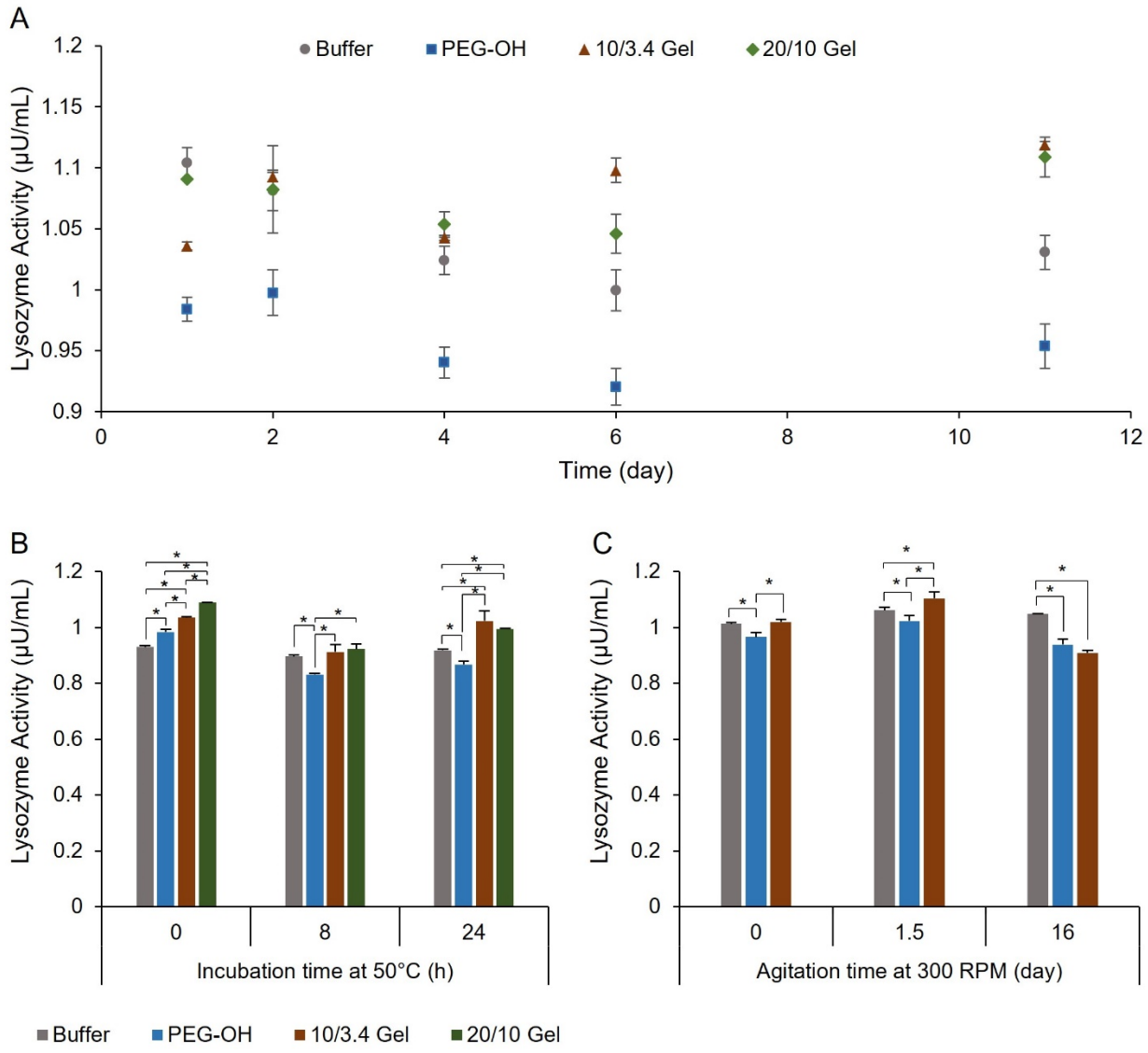

Figure 8: Lysozyme activity over time. A) Lysozyme activity as a function of time when incubated with buffer (PBS, free solution), in PEG-OH (crowding environment), or in 10/3.4 and 20/10 gel (confinement). Lysozyme activity as a function of time when subjected to heat 50 °C **(B)**, and mechanical agitation **(C)**. * denotes statistical significance ($p < 0.05$, n = 3).

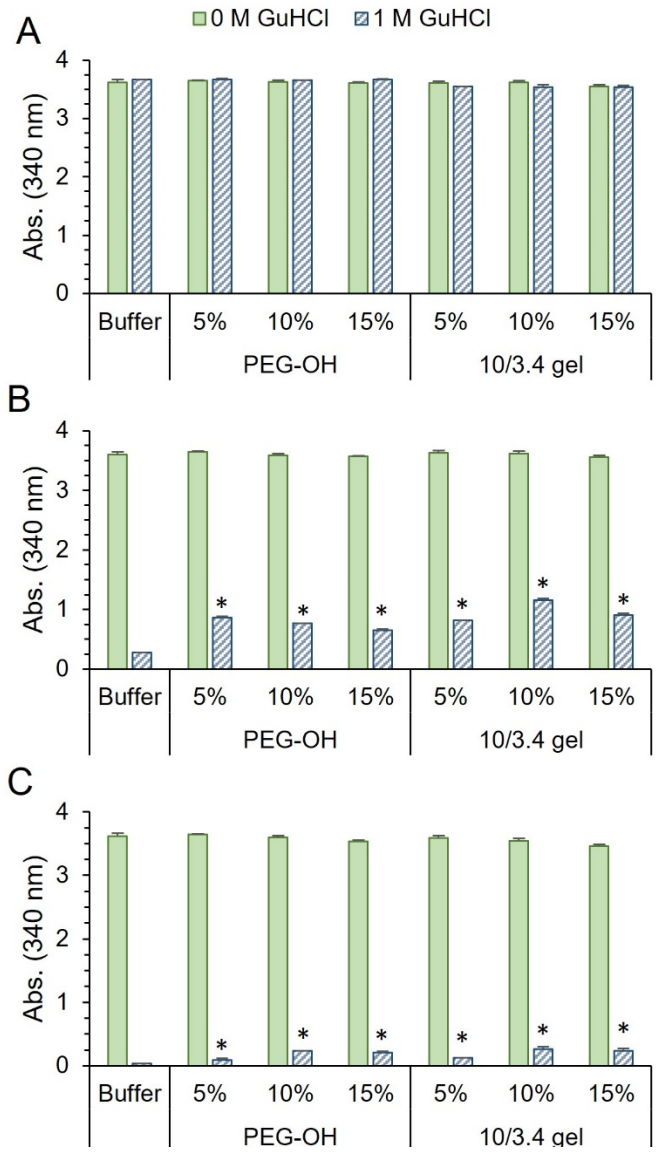

Figure 9: Alcohol dehydrogenase activity over time. ADH activity as a function of time when incubated with buffer (free solution), in 5 – 15% w/v PEG-OH (crowding environment), or in 5-15% w/v 10/3.4 (confinement) after **A)** 0 days, **B)** 2 days, and **C)** 6 days. * denotes statistical significance from buffer ($p < 0.05$, n = 3).